Chapter 3

On the magnetic field in Cometary Globules

3.1 Introduction

Massive stars have significant influence on the evolution of the ISM in their vicinity. Systems of bright rimmed clouds with head-tail morphology called the Cometary Globules (CGs) are found near massive stars (Schneps, Ho and Barret 1980; Zealey *et al* 1983; Reipurth 1983; Gyulbudagyan 1985; Sugitani, Fukui and Ogura 1991; Block 1992). The Gum-Vela region has a sizable population of $\sim$ 32 of these clouds. Recent studies have established that this region is a good example of the various effects of massive stars on their environments (Reipurth 1983; Sridharan 1992a,b; Sahu 1992). The Gum globules have the following characteristics:

- A compact head.
- A long faintly luminous tail extending from one side of the head; the other side has a sharp edge with a narrow bright rim.
- Sometimes the heads have embedded young stars in them.

The CGs are part of a larger family of dark clouds including the *elephant trunk globules, globular filaments and isolated dark globules* (Leung, 1985). They are found in various parts of the sky, the Orion Nebula and Rosette Nebula being two examples. CO maps of the Orion Nebula show globules with head-tail structure pointing away from the Orion OB1 association, a configuration similar to that seen in the Gum-Vela region. As discussed in the previous chapter, recent observations have established that individual systems of CGs are expanding away from

central massive stars possibly due to the *rocket effect* (Sridharan, 1992a,b; Indrani and Sridharan, 1994; Patel, Xie and Goldsmith, 1993) and that star formation is going on in some heads (Pettersson, 1991 and references therein; Sahu and Sahu 1992) at enhanced efficiencies (Bhatt, 1993; Ramesh, 1995). These results are in general agreement with the theory developed by Bertoldi (1989) and Bertoldi and Mckee (1990) for clouds exposed to ionising radiation. However, the role of magnetic fields in the formation and evolution of these clouds, as well as star formation in them, has not been adequately addressed. As elaborated below, this was the motivating factor for the study described in this chapter.

3.1.1 Motivation for our investigation

Several hypotheses have been put forward to explain the morphology and other properties of the Cometary Globules and similar clouds seen in the vicinity of HII regions. It is commonly assumed that these structures form from *density inhomogeneities* in a parent molecular cloud. For example, the elephant trunk globules are long tongues of neutral gas attached to a larger cloud complex, generally pointing towards the exciting star in an HII region. They could have formed when a shell of molecular and atomic gas, driven by an expanding HII region or stellar winds, encounter a condensation or clump in the ambient medium (Pikelner and Sorochenko, 1974). These structures could also be formed when instabilities develop in a wind-driven shell (Schneps, Ho and Barret, 1980), although Kahn (1958) has argued against this. Cometary Globules have also been proposed to form from pre-existing condensations which have survived the disruption of the parent cloud. Reipurth (1983) has proposed the following scenario for the Gum globules. When the massive star ζ Puppis started its main sequence life, its UV radiation disrupted the neighbouring clouds and separated the denser and less dense material. The cloud cores are thus exposed and will for a time show bright rims, and faintly luminous tails in the *shadow region.* In the shadow region, where the direct radiation from the star does not penetrate, the tail consists of eroded material from the core and left-over material from the cloud. Star formation could have ocurred at several stages: First, before the O star ignited; second, following the penetration of the ionization front in the thin outer part of the cloud; third, in the outer part of the globule itself; and fourth, in the center of the cloud following a radiation induced collapse.

The other major scenario to explain the morphology of these structures is that of radiation induced collapse (Bertoldi, 1989 and Bertoldi and McKee, 1990).

Here the cometary shape of the clouds results from their exposure to the UV radiation from the nearby massive star and subsequent collapse. The major parameters in this scenario are: the column density of the cloud and the density of the ionising radiation field relative to the cloud density. Clouds with small column density and/or those close to the ionising star are instantly ionised and expand into the intercloud medium. In clouds where the ionisation front slows down to develop a shock front before it reaches the back of the cloud, only a part of the initial mass is lost during the subsequent ionisation driven implosion. The remaining cloud gets highly compressed as the ionisation-shock front focusses the neutral shocked gas onto the symmetry axis of the cloud. This post implosion cloud then settles down to an equilibrium configuration, slowly evaporating while accelerating away from the star. These equilibrium configurations show a *cometary structure*. However, according to Bertoldi and McKee, this scenario is likely to apply only to the smaller "speck" globules (tear shaped clouds) seen in the Gum region and other HII regions and not to the larger cometary globules. Certainly the long tails (sometimes several parsecs as in CG 22) of these large globules cannot be explained as resulting from radiation induced collapse. These globules are likely to be in the very early phase of the evolution described above, just after the host cloud has disrupted.

Most of these scenarios, however, do not satisfactorily account for magnetic fields in these clouds. The theory of Bertoldi and Mckee treats magnetic fields only approximately and observational efforts in this direction have been limited. Hodapp (1987) studied three globules believed to be associated with expanding interstellar shells and found magnetic fields which he interpreted in terms of interaction with the shells. These globules however do not show clear head-tail morphology.

The CGs in the Gum-Vela show a variety of structures ranging from narrow filaments in the tails with aspect ratios as high as 10 (as in CG 22) to those that can hardly be called tails (as in CG 13). Tails which bend gradually (CG 1) or abruptly (CG 8) are also seen. The obvious question is what controls the morphology of the tails? Though the massive central star(s) can account for the presence and the overall radial orientation of the tails, the fine structure and the variety appear hard to explain. In particular we noticed the following problem: *from* CO *measurements we know that the linewidths which presumably represent turbulent motion are as much as the systematic velocity differences seen over the lengths of the tails* (Sridharan, 1992a). *If, as has been suggested, the*

systematic velocity gradients stretched the clouds to form elongated structures, why has the velocity dispersion not caused the dispersal of the clouds in directions perpendicular to the tails? The CGs are not gravitationally bound; their masses derived from CO maps are significantly smaller than those required for virial equilibrium (Harju *et al.*, 1990; Sridharan, 1992b). Radiation and stellar wind from the central stars may quickly sweep material getting out of the head-shadow region but this cannot explain structures narrower than the tail often seen in the CGs. With a velocity dispersion of ~ 1 km/s and typical widths of the filaments of $\sim 1'$ the lifetime of these structures will most likely be $\sim 10^5$ years, much shorter than the dynamical ages of the CGs of a few million years. This implies that *either these structures are transient or there is a restraining agent which channels the flow in the tails.* Magnetic fields aligned along the tails can confine gas and may also explain the bent tails.

One of the globules studied by Hodapp (1987), ESO 210-6A, is in the Gum-Vela region. Though not classified as a Cometary Globule (Reipurth, 1983) it shows magnetic field pointing towards the central region of the system of CGs. The location of the globule is such that the direction to the central region is roughly parallel to the Galactic plane. Therefore it is not very clear whether the field detected by Hodapp is of general interstellar origin (parallel to the Galactic plane) or associated with the globule in question.

Motivated by these questions we started a program to study possible magnetic fields in the CGs. In this chapter we report the detection of magnetic field along the tail of CG 22 by studying *the polarisation of starlight passing through it*. This globule is the largest of the CGs and shows streaky filaments well reproduced in CO maps and has two condensations along its tail which may actually be separate objects.

Before describing our observations, we digress to discuss magnetic fields in our Galaxy and the tools used to study them, with emphasis on optical polarisation studies.

3.2 Magnetic fields

Magnetic fields are present in all the major components that make up the Galaxy: stars, interstellar gas, dust etc. As to the origin of these fields, it is generally accepted that they are amplified from insignificant primordial fields to their present values by the inductive effect of fluid motions (for a review of the theories of origin

and the observational status, we refer to Parker, 1979; Zweibel and Heiles, 1997). The field energy can be increased in this fashion upto approximate equipartition with the turbulent energy. This is indeed what observations seems to bear out. However, the serious difficulty with this picture is the increased tangling of field lines that is implied in the near absence of magnetic diffusion (which is the case in the ISM where the ohmic resistivity is extremely low). The measured mean interstellar field is of the same order as the r.m.s field, indicating that there is no extreme tangling of the field, contrary to the prediction. To avoid this impasse, one can appeal to turbulent diffusion, which can be orders of magnitude higher than ohmic diffusion. The magnetic forces acting on the fluid could also resist configurations which lead to field cancellation (for example, field lines twisting back on themselves). This in turn would reduce the extent of entanglement. The two leading theories for origin and maintenance of the magnetic field are the *dynamo theory* and the *amplification of the primordial field.*

In the dynamo theory, the mean interstellar field (B_μ)is produced by the action of large scale (e.g., galactic rotation) and small scale (turbulence) fluid flows. In its simplest form, the theory predicts exponential growth of some dominant mode of the magnetic field with time. The effect of the field itself tends to "quench" the dynamo when equipartition is reached with the turbulent energy and B, saturates at this value. The galactic disk dynamo generates predominantly azimuthal fields through strong shear by Galactic rotation and have quadrupolar symmetry. The field produced is axisymmetric (see Fig 3.1).

The primordial theory postulates a large scale field of microgauss strength at the time of formation of the galaxy. Again, resistivity is neglected. Differential rotation wraps the field into a bisymmetric spiral. Differential rotation makes the azimuthal component predominate and reverse in direction with radius. The approximate equipartition with turbulent energy is not explained by the model, but could be explained by buoyancy instabilities which occur if the field becomes too large and limits it to the equlibrium value.

The observational tests for these theories are usually the direction of the vertical field component, which has opposite polarities for the two theories and the azimuthal symmetry, which is axisymmetric for the dynamo and bisymmetric for the primordial theory. At present, both theories remain viable with existing observations being unable to definitively confirm one or the other.

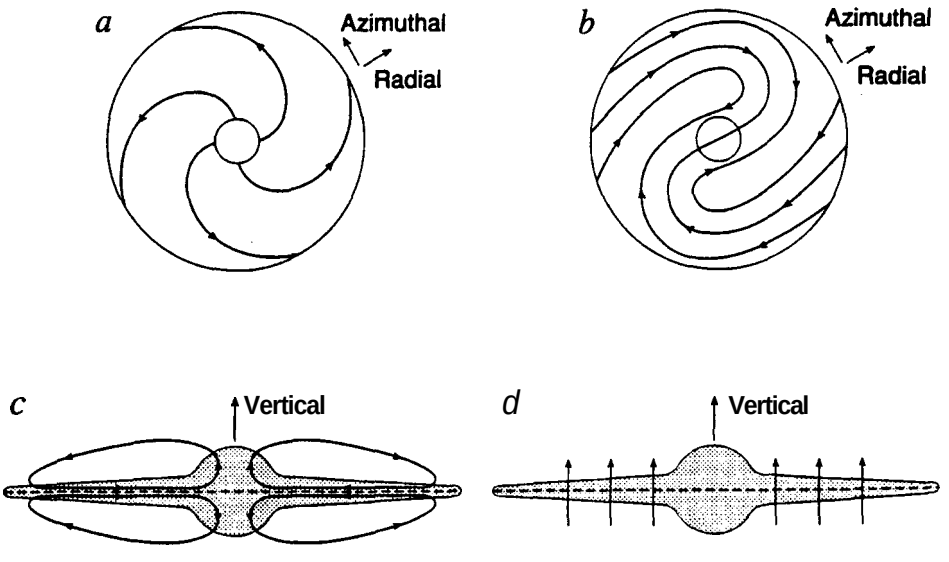

Figure 3.1: Sketches of the magnetic field configurations in disk galaxies according to various models. The bold lines are magnetic field lines, with field direction indicated by arrows. **a:** Face-on view of axisymmetric spiral structure. **b:** Face-on view of bisymmetric spiral structure. c: Edge-on view of quadrupolar (even parity) magnetic structure. **d:** Edge-on view of odd-parity magnetic structure. From Zweibel and Heiles (1997).

3.2.1 Observational techniques

Observational tracers of the magnetic field are responsive to either the plane of the sky component ($B_\perp$) or the line of sight component ($B_\parallel$). The field has a uniform component (B,) and random component (B_r) with the total field $B_t^2 = B_u^2 + B_r^2$.

1. Polarization of starlight. The very existence of the interstellar magnetic field was inferred from the linear polarisation of starlight. The polarisation is produced by the alignment of dust grains in the magnetic field. The polarisation produced is parallel to $B_\perp$ namely, the projection of the field on the plane of the sky. In this chapter, we use this probe to map the field in a Cometary Globule. We describe this technique and the cause of polarisation in greater detail later. For completeness we mention the other techniques below.

2. Linear polarisation of synchrotron radiation. Synchrotron radiation is produced by the gyration of relativistic electrons in a magnetic field. The direction of polarisation is parallel to the direction of acceleration and so the polarisation is perpendicular to the magnetic field, i.e the observed polarisation is perpendicular to $B_\perp$. In the actual case, the interstellar field has both $B_\perp$ and $B_\parallel$ component. The strength of polarisation of the synchrotron radiation goes to zero if the field is completely along the line of sight, but the observed polarisation is always perpendicular to $B_\perp$. The random component, by definition, has net polarisation zero. If the angle between the line of sight and B_u is known, the ratio of B_r to B_u can be obtained from the degree of polarisation.

3. Faraday rotation. The Rotation Measure

$$RM \propto \int n_e B_\parallel \tag{3.1}$$

where n_e is the electron density and the integration is over the path length, is derived from the Faraday rotation of the plane of linear polarisation of a background radio source. Along the line of sight, all electrons rotate clockwise or counter-clockwise depending on the direction of the magnetic field producing a difference in phase velocities for the two senses of circular polarisation. The combination of the two circular polarisations with a specific phase difference produces a net linear polarisation of a specific position angle. Since the phase difference acquired depends on the wavelength, so does the position angle of the linear polarisation. It is proportional to RM x λ^2 (Spitzer, 1978). The n_e has to be estimated to get $B_\parallel$ from the Faraday rotation.

The RM can be measured for pulsars, and in combination with the dispersion

measure DM $\propto \int n_e dl$ (which can also be measured for pulsars) provides the magnetic field strength unambiguosly.

4. **Zeeman splitting.** To take the example of the hydrogen atom, an external magnetic field splits the upper level of the 21 cm line into three levels. The splitting $\nabla\nu$ between the highest and lowest levels is $2.8B_t$ Hz, where B_t is the total field strength in μG. The atom radiates two circularly polarized a components separated in frequency by $\nabla\nu$ with maximum amplitude parallel to the magnetic field and three linearly polarized π components with maximum amplitude perpendicular to the magnetic field. In *diffuse* clouds, the splitting is much smaller than typical line widths and the components cannot be distinctly separated. The splitting is detected by observing the *difference* between the circular (Stokes parameter V) or linear (Stokes parameter Q and U) polarisations. Given the small $\nabla\nu$, the π components are virtually undetectable. The observed amplitude of the Stokes V spectrum a components is proportional only to the parallel component of the magnetic field.

The two techniques for measuring $B_{||}$ typically sample two kinds of regions. Zeeman splitting favours high HI column density and narrow line width and so traces cold HI clouds, whereas Faraday rotation samples ionized regions.

3.2.2 The observed Galactic field

Deatiled observations of the line of sight component through Faraday rotation of radio sources and pulsars and Zeeman splitting measurements are available for the Milky Way. Large scale optical and radio polarisation maps provide the orientation of the field in the plane of the sky. Rough information on the large scale behaviour of magnetic field strength is obtained from models for the all-sky brightness of the diffuse Galactic synchrotron emission (see Kulkarni and Heiles, 1987 and references therein). The local interstellar magnetic field strength is estimated at -3 μG from synchrotron emissivity. The strength obtained from pulsar Rotatiom Measures and Dispersion Measures is lower and is of the order of $\sim 1.6\mu$G. Persuasive arguments based on the magnetic component of the pressure required to support the observed thickness of gas in the disk lead to higher estimates for the interstellar field (Boulares and Cox, 1990) of the order of ~ 5 μG. Recent observations are starting to vindicate this point of view (Heiles, 1995).

As regards the direction of the field, large scale optical polarisation maps reveal that the field lines lie *parallel* to the plane of the Galaxy. As seen in Fig **3.2,** the comprehensive map from Axon and Ellis (1976) illustrates this. We recall

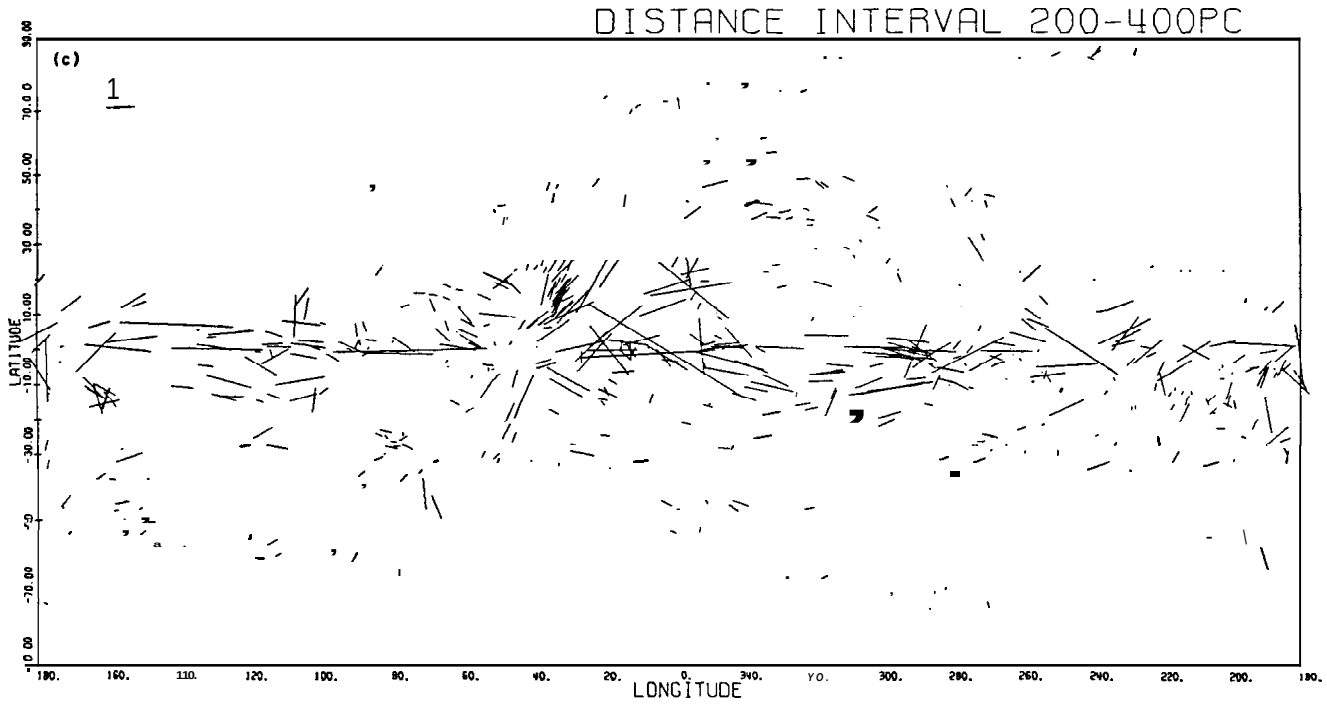

Figure **3.2:** The polarisation of starlight along the plane of the Galaxy from Axon and Ellis (1976). The mean field lies along the plane as seen from the average distribution of polarisation vectors. The length of each line is proportional to the percentage polarisation according to the scale marked in the top left hand corner. The map contains all stars which are at distances between 200 and 400 pc.

this while discussing the field in CG 22. The optical data also indicates that the field is roughly circular as in external galaxies. However, Rotation Measure data from the solar neighbourhood indicate the existence of one or more field reversals within the solar circle although alternative explanations exist.

Since this chapter deals with a study of the magnetic fields in a molecular cloud, we briefly discuss the observed fields in both diffuse and dense clouds. Optical polarisation data shows that the magnetic field often lies parallel or perpendicular to HI filaments and elongated HI clouds. The North Polar Spur, a giant radio loop with an associated HI shell, is a spectacular example (Heiles and Jenkins, 1976). However, the strength of the magnetic field does not seem seem to increase with the density of the clump or clouds. Magnetic field strengths show no sign of increase over density ranges 0.1 to 100 cm^{-3} (Kulkarni and Heiles, 1987). Although magnetic field enhancement is not expected if these condensations form by quiescent streaming of gas along field lines, shocks would certainly increase the field strengths and hence some enhancement is expected. The field already dominates in the dynamics and pressure equilibrium of clouds, so a significant increase in field strength with density is not likely.

In molecular clouds optical polarisation of background starlight has been used to look at field orientation, though this technique is often necessarily limited to the peripheral regions of the cloud where the extinction is less. Although in some regions the field does seem to be related to the cloud elongation recent results seem to indicate that if one looks at entire molecular complexes and large clouds, the orientation does not seem to be related in any special manner with cloud structure (Goodman, Myers and Bastien, 1990). Zeeman splitting of OH masers, polarisation of emission and absorption lines in the presence of magnetic field etc have given a great deal of information of the field in dense clouds. Whether the field traced inside clouds by masers is indicative of the overall field is still not clear. The Orion cloud complex and the Bl cloud in Perseus are examples of clouds extensively studied for magnetic fields. For a review of these and other results, we refer to Heiles et *al.*(1990). The field strength in general varies from ~ 0.05 to $\sim 40 mG$ for densities in the range $\gtrsim 400$ to $\sim 10^9 cm^{-3}$, indicating very roughly that $B \propto n^{1/2}$. The milligauss fields are limited to the "masing" regions. The average field strengths vary from 15 to 125 μG or so.

3.2.3 Alignment of grains

As mentioned before, optical polarisation provided the first clue for the existence of the interstellar magnetic field. The polarisation is produced by preferential extinction by elongated dust grains which are aligned by the magnetic field. The preferred mechanism for alignment is one which was originally proposed by Davis and Greenstein (1951). The dust grains are constantly colliding with atoms of interstellar gas which make them spin. If they are in collisional equilibrium, the energy of spin is equal about all the three principal axes. This means that the maximum angular momentum is about the axis of largest moment of inertia. The dust grains usually end up spinning end-over-end. The spinning dust grain sees a time-varying magnetic field. Under these circumstances, two energy-dissipation mechanisms are relevant. One is due to the induced electric currents in the grain. The other, and more important one under interstellar conditions, is because of the magnetic susceptibility of the grain. The induced magnetic moment $\vec{M}$ exerts a torque on the grain

$$\vec{L}_c = \vec{M} \times \vec{B} \tag{3.2}$$

where $\vec{B}$ is the external field. This causes the angular momentum $\vec{J}$ of the grain to precess about $\vec{B}$. Therefore, regardless of alignment, the average orientation of the grain is controlled by 8, since the angular distribution of the orientations is rotationally symmetric about 8 . *Observations suggest that the grains are aligned perpendicular to* $\vec{B}$. The imaginary component of the complex susceptibility represents the absorption of energy because of the constantly changing magnetic field in the material. This results in a difference in alignment between the induced field inside the grain and the external field. The imaginary part of the susceptability constantly drags the induced field in the grain along with the material and away from B. It effectively produces a magnetic moment perpendicular to the external field. This obviously exerts a retarding torque on the grain. This retardation drives the grain towards a configuration where *it is spinning with the spin axis parallel to the external field, i.e in the case of a needle like grain, it spins with the short axis along the magnetic field.* This results from the fact that the retarding torque is independent of the moment of inertia (see Spitzer 1978) and so as the grain nutates, varying the angle between each principal axis and B, the rotational velocity about axes of relatively lower moment of inertia tend to damp out earlier. If the spin-up of the grain itself makes the grain rotate about its short axis, then the observed alignment is explained at least qualitatively. Otherwise, the process of magnetic relaxation described above produces the alignment. The final con-

figuration of the spinning grain is shown in Fig 3.3. The time-averaged projected length of the grain is longer in the direction perpendicular to the magnetic field. This results in preferential absorption of the $\vec{E}$ vector of the passing light wave and produces a resultant polarisation.

The original Davis-Greenstein mechanism had the grains rotating purely as a result of collisions. But this requires very high magnetic fields to produce the observed polarisation. A modification of the theory by Purcell (1979) requires much lesser field strengths. According to this theory the grains have much higher spin energies; they have supra thermal rotation. The spin is caused by ejection of hydrogen molecules from preferred sites on the grain (like "jets" on a pinwheel). The grain therefore experinces an unbalanced, time averaged torque causing it to rotate as fast as upto an w of $10^9 s^{-1}$. The other alternative is that the grains are super paramagnetic or even ferro-magnetic causing alignment even in weak fields.

3.3 Observations

The observations described here were carried out with a fast star and sky chopping polarimeter coupled to the $f/13$ Cassegrain focus of the 1-m telescope at the Vainu Bappu Observatory, Kavalur on the night of March 6, 1995. A detailed description of the instrument and the method of data reduction may be found in Jain and Srinivasulu (1991). We briefly summarize the observation and analysis technique.

For most astronomical sources, the degree of polarisation is very low and measuring the polarisation involves measuring the small difference between two large intensities. The instrument we have used rapidly alternates between the star and the neighbouring sky in order to minimise errors, hence the name star-and-sky chopping. The state of polarisation is completely described by the four Stokes parameters I, Q, U and V. I is the mean intensity, Q represents the difference between intensities transmitted through two mutually orthogonal positions of an an analyzer, U is the difference between 45" and 135° positions (with reference to the axes used for Q) of the analyzer and V is a measure of the handedness of circular polarisation. To measure linear polarisation, the intensity of transmitted light at a minimum of three positions separated by 45" needs to be measured. In practise, this is done at many positions by rotating the analyser in the path of the incoming beam. The intensity at position a (the angle between the incident

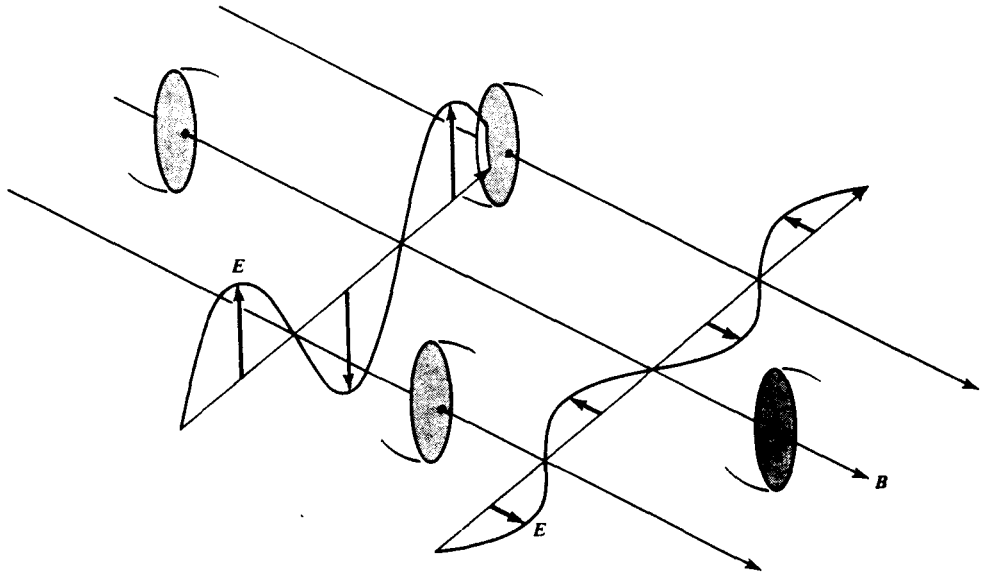

Figure **3.3:** The alignment of a spinning dust grain in an external magnetic field. The grain spins with its average projected length being longer perpendicular to the plane-of-sky magnetic field. As shown, this causes the $\vec{E}$ vector of the passing light wave to be preferentially absorbed perpendicular to the field. The resulting observed polarization is thus parallel to the field. From Shu (1986).

light elctric vector and the transmission axis of the analyzer) is

$$I(a) = \mathrm{I}\cos^2\alpha \qquad (3.3)$$

The intensity versus angle of the analyzer curve is a double sinusoid. A least squares fit to the amplitude and phase of the sinusoid gives the amplitude and position angle of the polarisation. The main sources of error are photon noise, atmospheric scintillation and "seeing", variable sky background and instrumental polarisation. Longer integration obviously reduces the photon noise. The atmospheric seeing causes the image of the star to move about on the surface of the photomultiplier tube. The non-uniform response of the tube (intrinsic to all photo tubes) causes the output current to fluctuate. This is overcome by imaging the *primary mirror* of the telescope instead of the star image onto the tube, using a Fabry lens. The errors due to scintillation and variable sky are reduced by rapid modulation of the signal and *switching* between the adjacent sky and the star at a fast rate. The incoming starlight after passing through a rotatable anlyzer is focussed on one of two identical focal plane diaphragms and the neighbouring sky is focussed on another. A metallic plate with two semicircular slots in it is rotated in front of the diaphragms so that the light from the star and sky is chopped alternately. The light then passes through filters and is focussed by the Fabry lens onto the photo tube. The instrumental polarisation is calibrated out using standard calibrator stars.

Briefly, the star and the neighbouring sky 2′ away are observed alternately every 20ms for 200 positions of the analyser. A function of the form $A + B\sin 2\theta + C\cos 2\theta$ is fitted to the (star - sky) difference data by least-squares to obtain the intensity, and the percentage and the position angle of the linear polarisation of the star light. An unfiltered dry-ice cooled R943-02 Hamamatsu photomultiplier tube was used for the measurements. Thirteen stars brighter than ~ 13 mag were observed with integration times of 5 - 10 minutes. An aperture of 30" diameter was used. The stars chosen were distributed over the head and immediately following tail region of CG 22; the two clumps further down the tail were not covered. The instrumental polarisation was determined by observing unpolarised reference stars from Serkowski (1974) and was found to be $0.17 \pm 0.026\%$. The zero of position angle was determined by observing polarised standards from Hsu and Berger (1982). The results have been appropriately corrected for these effects.

Table 3.1. Summary of observations

No.	mag (R)	%P	$\%\epsilon_P$	θ (°)	ϵ_θ (°)
1 (SAO199273)	9.0	0.54	0.10	139.1	10.5
2	9.7	0.29	0.14	16.2	
3	10.2	0.44	0.16	13.3	20.3
4 (Wra 220)	11.6	1.58	0.45	37.7	16.2
5 (SAO199269)	9.0	0.16	0.10	164.0	
6	10.5	1.16	0.19	4.4	9.4
7	8.4	0.36	0.08	145.1	12.8
8	10.0	0.83	0.13	30.3	9.1
9	10.5	0.96	0.19	16.6	11.6
10	9.2	0.54	0.13	25.1	13.6
11	10.6	0.84	0.29	52.8	19.8
12	10.7	0.43	0.24	59.6	
13	11.3	1.28	0.31	26.3	13.9
b1		0.25	0.06	112.7	6.8
b2		0.27	0.07	136.2	7.2
b3		0.56	0.10	115.9	4.8

Table 3.1: Summary of observations: Column 1 lists the identification of the star. The numbers are as indicated in Fig 3.5. b1, b2 and b3 refer to the three stars in the region $\sim 3°$ northeast of CG 22 from a separate survey (Bhatt 1995). Column 2 lists the magnitude of the stars which are roughly equal to the Johnson R band magnitudes. Stars 1, 4 and 5 have been used to calibrate the magnitude scale. The error on magnitudes is ~ 0.5. Column 3 lists the percentage polarisation and 4 the error on this quantity. Column 5 gives the position angle of polarisation measured from north increasing towards east. Column 6 shows the error on the position angle. The errors are derived from the least squares fit.

3.4 Results

The results of our observations are presented in Table 3.1. The magnitudes of the stars observed were obtained from the mean intensity. The photocathode response may be considered to approximate the Johnson R band. Stars 1 and 5 are indentified to be SAO 199273 and SAO 199269. Star 4 is identified with the Ha emission star Wra 220, which is same as PHα92 and has also been detected at 2.2μ, 50μ and 100μ (Reipurth, 1983; Pettersson, 1987; Sahu and Sahu, 1992). We have used these three stars to calibrate the magnitude scale. The likely errors are ~ 0.5 mag. The stars b1, b2 and b3 from a separate survey (Bhatt 1995) are in the Gum-Vela region $\approx 3°$ north-east of CG 22. The position angles listed are measured from north, increasing towards east. The errors given are obtained

from the least-squares fits. Fig 3.4 shows the polarisation vectors on an optical picture of CG 22 (from SERC "*J*" survey plates), with the CO contours (from Sridharan 1992b) also plotted. The lengths of the vectors are proportional to the percentage polarisation and the orientation is same as that of the $\vec{E}$ field.

3.5 Cause of the polarisation

We have plotted in Fig 3.5 the polarisation position angle against the percentage polarisation for all the stars with detected polarisation. The plot shows two clearly separated groups of stars, with *low polarisation* having position angle $\sim$ 140° and roughly parallel to the the Galactic plane (group 1) and *high polarisation* showing position angles near 30° which is roughly the direction of the tail (group 2). We suggest that the origin of the polarisation in the two groups are due to dust grains aligned by magnetic fields in the general ISM and in CG 22 respectively. This is because the stars in the two groups also occupy different regions with respect to the boundary of the cloud as further discussed below.

From Fig 3.4, we see that stars 1,2 and 5 which are outside the cloud in projection show polarisation characteristics distinctly different from the other stars seen projected on the cloud. Polarisation was not detected in light from stars 2 and 5 within our errors of measurement, and star 1 shows small percentage polarisation oriented very differently compared to the other stars. All the stars projected on the cloud except 12, have larger polarisation with orientation parallel to the tail and fall in group 2. Star 12 shows no polarisation even though it is within the cloud boundary. This may be due to this star being in the foreground of the cloud. From optical pictures it is difficult to say whether stars 7 and 11 are within the cloud boundary or not. We note that the detection on star 11 is less than 3 sigma. However, the direction of polarisation is similar to those of the other stars projected on the cloud. The detection on star 7 is better than 4 sigma and its direction is similar to that of star 1 which is outside the boundary. This direction is roughly parallel to that of the Galactic plane (145°). The direction of polarisation caused by general interstellar dust being parallel to the Galactic plane (Mathewson and Ford 1970, see section 3.2.2), we conclude that the polarisation of the light from the stars 1 and 7 may be due to the general interstellar dust. The polarisation position angles of stars b1, b2 and b3 further support this. Stars 2 and 5 show no polarisation presumably because they are closer than stars 1 and 7.

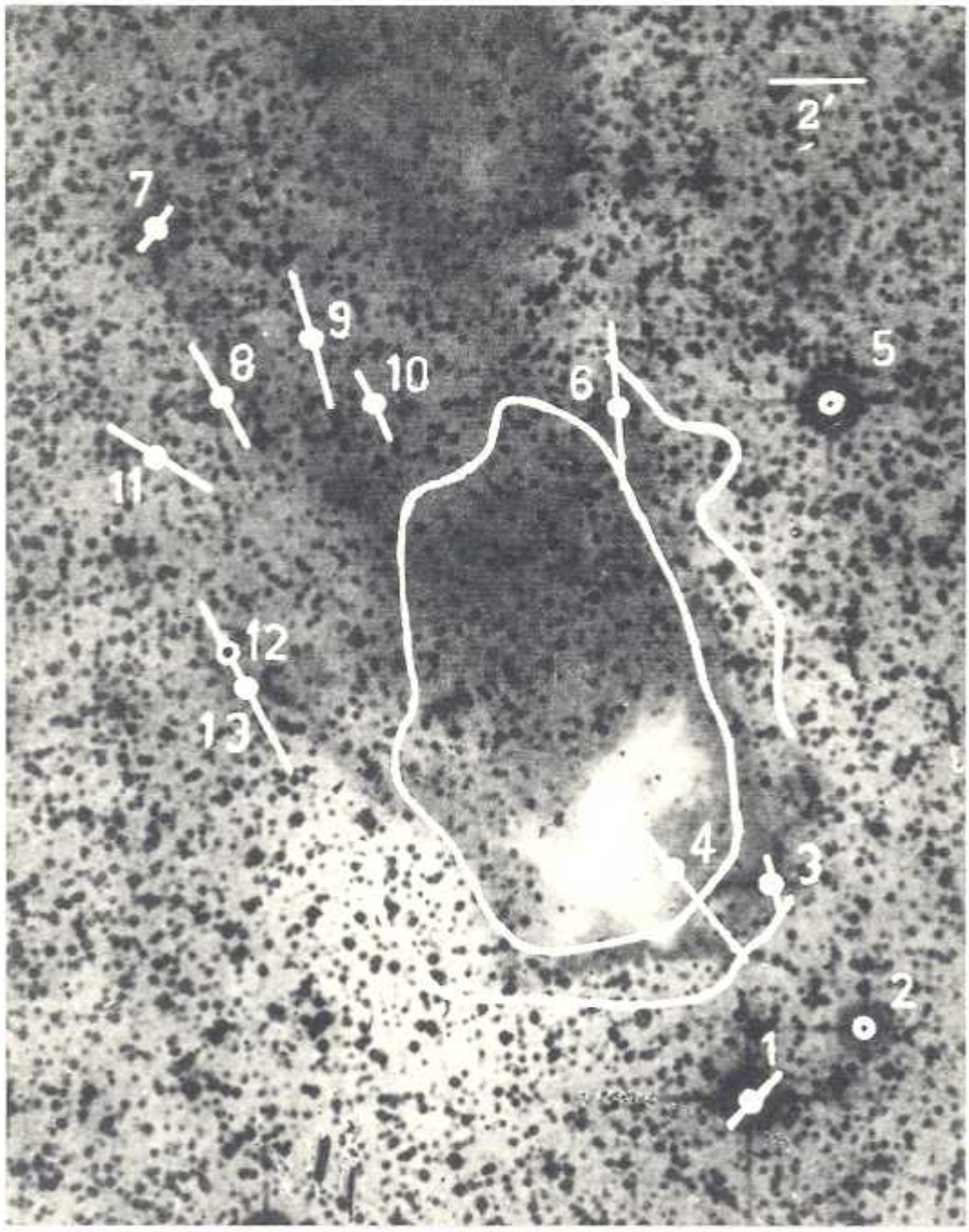

Figure 3.4: Polarisation of stars seen projected on and near CG 22. The lengths of the vectors are proportional to the percentage polarisation and the orientation is same as that of the $\vec{E}$ field. Polarisation vectors have been plotted only for those stars with detections better than or close to 3σ and non-detections are marked by circles. CO contours from Sridharan (1992b) are also shown on the SERC survey picture. The inner contour corresponds to a T_{kin} of 10K and the outer contour represents the boundary. The cloud was not fully mapped on the northern side where a condensation along the tail is seen.

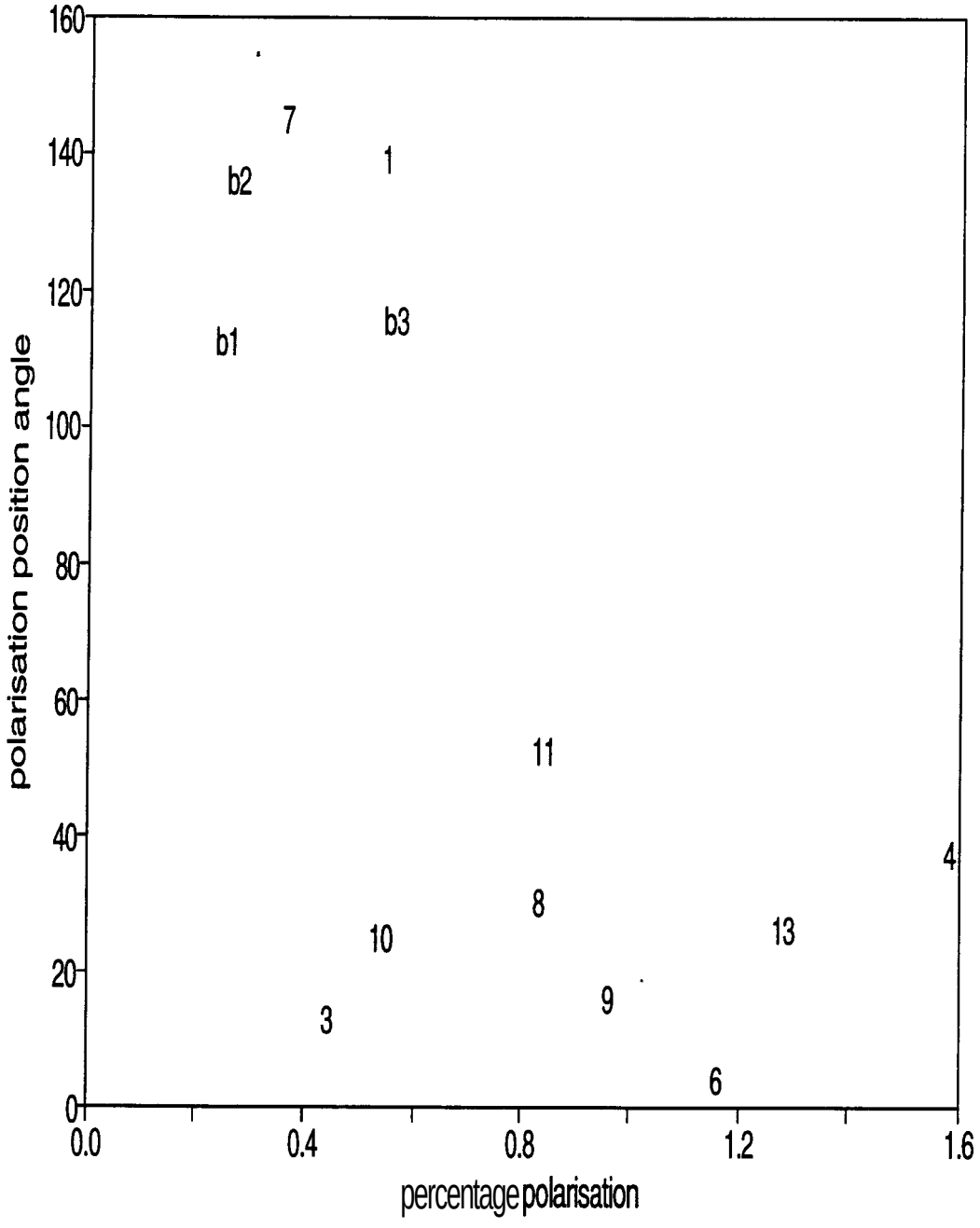

Figure **3.5:** A plot of polarisation position angle against percentage polarisation. The plot shows two groups of stars, with low polarisation having position angle $\sim 140°$ and high polarisation showing position angles near 30°.

For stars in group 1, the amount of polarisation is $\sim 1\%$ which implies a P/A_V ratio of ~ 1, using extinction data (~ 1 mag) from Sahu *et al* (1988). This value is in agreement with measurements towards other clouds and in the general ISM where the polarisation is believed to be caused by dust grains aligned by magnetic fields.

We recognise that the measurement of polarisation of star-light in this region is complicated by the fact that the tail may be a reflection nebulosity and hence may contribute polarised light over the aperture used. We argue below that the observed polarisation is unlikely to be due to this. The peak optical surface brightness anywhere over CG 22 is ~ 23.7 mag/arcsec^2 in the "J" band (from the SERC "J" plates whose pass band ranges from 395 - 540 nm; Sahu *et al.* 1988). If the optical nebulosity is due to reflection it is likely to peak in the "J" band. In the R band, which the photocathode approximates, the surface brightness is likely to be less. Over the aperture used (30″ diameter) we estimate that the nebulosity will contribute light equivalent to 16.6 mag. If this light is 100% polarised, we estimate that it can result in 1 % polarisation for stars fainter than 12.4 mag, assuming no chopping. The star/sky chopping will remove much of the light due to the optical nebulosity and only brightness gradients over 2' angular scales will contribute and this will be much less. As the faintest star on which we have detected polarisation is 11.6 mag (star 4), we conclude that our polarisation measurements are not contaminated by contribution from possible reflected light. The fact that star 12 showed no detectable polarisation supports this. Further the observed orientation of the polarisation vectors, if due to reflection, indicate a direction for the source of light towards a region where there are no bright stars.

From the above arguments we conclude that the polarisation of light from stars seen projected on CG 22 is due to selective extinction by dust grains aligned by magnetic fields in this cloud.

3.6 Discussion

3.6.1 The Strength of the Magnetic Field

If the polarisation is due to non-spherical dust grains aligned by a magnetic field, the polarisation position angles also represent the orientation of the magnetic field projected on the sky. *Orientation of dust grains by flow along the tail will cause polarisation perpendicular to what is seen.* Assuming alignment by magnetic field, **our results imply that the plane of the sky component of the**

magnetic field in CG 22 is oriented parallel to its tail. The mean value of the position angles is 22.5" with an rms dispersion of 5° (1σ). The tail itself shows a total variation in position angle of $\sim 30°$. There is an indication of the B-field orientation following this variation but more accurate data is needed to confirm this. It appears reasonable to conclude that the magnetic field is quite tightly aligned to the tail in three dimensions. Similar observations towards ESO 210-6A, a globule with wind-blown appearance in the Gum-Vela region, made in the near IR by Hodapp (1987) have resulted in the detection of a magnetic field pointing towards the central region. As already mentioned in the introduction, in the case of ESO 210-6A, this field could also be of general interstellar origin, whereas for CG 22 our data establishes the presence of a field aligned to the tail. In two other globules Hodapp has found bent field structure near the head which is seen neither in ESO 210-6A nor CG 22 possibly because of the limited number of stars observed. Polarisation data on more CGs along with better coverage will be useful in establishing these conclusions.

As mentioned previously, the P/A_V ratio is similar to that in the general ISM. Following Greenberg (1978) the required magnetic field strength is given by

$$B^2 \sim 0.5 a n_H T_d T_g^{1/2} \tag{3.4}$$

where a is the average grain size in μm, T_d and T_g are the dust and gas temperatures respectively and n_H is the hydrogen gas number density. Using CO data from Sridharan (1992b) and IRAS data from Sahu et al. (1988) we obtain values for n_H, T_g and T_d to be ~ 200 cm^{-3}, 10 K and 30 K in the outer parts of the cloud. Assuming a $= 0.1$ μm gives a value of 30 μG for B. The values of the parameters going into this estimate are only approximate and there is uncertainty about the quantitative validity of the Davis-Greenstein mechanism for aligning the garins. We stress that this field strength is a rough estimate and is intended only to give an idea of the kind of fields involved. The energy density in such a magnetic field is $B^2/8\pi \sim 3 \times 10^{-11}$ ergs cm^{-3}. From the CO linewidths of $\sim$ 1 kms^{-1}, the energy density in gas motion is $\sim 10^{-11}$ ergs cm^{-3}. This suggests that the magnetic field may be important in deciding the gas motions. In other words it could be playing a role in confining the gas in the tail as suspected.

3.6.2 Polarisation of light from the star Wra220

The large polarisation measured on star 4, which is believed to be a T-Tauri star formed in CG 22 is interesting. Light from such young stars may have

intrinsic polarisation due to scattering by circumstellar structures like disks. The polarisation vector in such cases is known to be parallel to the disk (Bastien, 1987 and references therein). The orientation of the polarisation for this star is similar to the other stars, and therefore the disk if present must be oriented *parallel to the magnetic field in the tail.* On the other hand current theories of star formation suggest the formation of flattened circumstellar structures perpendicular to the magnetic field. This inconsistency can be reconciled if the field in the core is unrelated to the field in the tail. A similar conclusion was reached by Hodapp for the globules ESO 210-6A and L810.

If the polarisation is not due to such structures, it implies dust alignment deep inside the cloud where the star is presumably embedded. From CO data, the inferred n_H is $\sim 10^3$ cm^{-3} indicating a magnetic field strength of ~ 70 μG. Further observations to distinguish between these two cases will be very useful because of the implications to the origin of the aligned magnetic fields in the CGs. In the second case any mechanism seeking to explain the geometry of the field should be able to produce aligned fields deep inside the cloud.

3.6.3 Origin of the field

We make some tentative remarks about the possible origin of the aligned magnetic field. First we assume that the magnetic fields in general are aligned to the tails in all CGs which is consistent with our data on CG 22 and Hodapp's observations. This needs to be established in many more globules but we shall assume that this is very likely. Clearly, such a field could not have existed in the original molecular cloud from which the CGs formed. This is because, given the radial distribution of the CG tails, a pre-existing magnetic field would have to be already pointing radially in the molecular cloud which appears far fetched. It is more likely that processes that were responsible for the morphology of the CGs were also responsible for creating the aligned magnetic field, possibly from a pre-existing randomly oriented seed field. Tentatively, radiation pressure on charged dust grains could have resulted in these grains being accelerated along the tail stretching any pre-existing magnetic fields along the tail. Ionised gas flow along the tails will also lead to the stretching of the magnetic field. Dust grains in HII regions can have charges of $\sim 100e^-$ and the initial magnetic fields may not have been strong enough to prevent radiation pressure from pushing the grains. The theory of Bertoldi (1989) treats only special cases where the magnetic field is oriented either parallel or perpendicular to the symmetry axis. In both cases

their post implosion clouds have magnetic fields oriented in the same way as the initial cloud. In this picture, our results would imply an unlikely situation where magnetic fields parallel to the future tails are already present in pre-implosion clouds. Moreover, as mentioned in the Introduction, Bertoldi and McKee (1990) do not ascribe the morphology and tails of the large globules seen in the Gum region and elsewhere to the effects of radiation induced collapse. These large globules are likely to be in the very early stages of evolution, where the initial cloud has just been disrupted.

The measured field seems to favour the scenario that the head of the Globule is a pre-existing condensation, with the tail being either ablated clump material or leftover gas in the shadow region of the head. The alignment of the field parallel with the orientation of the Globule indicates the effect of radiation or gas flow past the Globule. We emphasise that the optical polarisation probes only the field at the periphery of the Globule. The head of the Globule shows a bright rim caused by radiation from the central star(s). In Chapter 4, we show that the ionized rim is almost certainly caused by ζ Puppis, the O4f giant in the vicinity. Recent Hipparcos distances confirm the proximity of this star to the CGs (see Chapter 2 for a detailed discussion). The material being ablated from the head could be swept back onto the tail forming a sheath of ionized material entrapping the field, which would be aligned by the gas flow. The velocity gradient seen along the tail in the CO emission line is still not satisfactorily explained. In Chapter 2 we argued that the environment of the CGs could be be the interior or edge of a shell of gas and dust being swept out of the ISM by the stars in Vela OB2, the OB association seen more or less centrally located with respect to the CGs. If this is so, the effects of stellar winds and swept-up gas flow past the CGs may be important. The resulting drag on the CGs could be the reason for the velocity gradient along the tail. The alignment of the field, at least near the boundaries of the CG could also be the result of of this flow. The star formation in the Globule is likely to be the result of the ionization-shock front moving into it.

At this point we would like to comment on a suggestion by Scarrot et. al. (1992) of a possible large scale magnetic field in this region parallel to the Galactic plane which influences star formation, leading to various aligned structures. The direction of the field they have assumed is from Hodapp's measurements towards ESO 210-6A. The magnetic field direction inferred from our data is $\sim$ 68 " away from that in ESO 210-6A and would appear inconsistent with this picture. However, the detected fields may be unrelated to those in the cores of individual

globules (Hodapp, 1987) whose orientations need to be measured to test Scarrot et. *al.*'s suggestion.

3.7 Summary

- We have presented results of linear optical polarisation measurements on stars seen projected on CG 22 in the Gum-Vela region.
- For stars within the cloud boundary we detect a polarisation of $\sim 1\%$ with position angle oriented parallel to the tail whereas those outside the boundary show either small polarisation with the position angle parallel to the Galactic plane or no polarisation within the errors of our measurements.
- a This implies that the field in CG 22 is aligned parallel to its tail.
- a A rough estimate of the field strength indicates that it may dynamically important.
- We suggest that the alignment could only have been caused by the same processes responsible for the formation of the tails.
- The alignment of the field suggests that the radiation from the central stars as well as gas flow past the globule could play a role in its evolution. This is of relevance to the scenario wherein the Globule is at the edge or in the interior of a shell of gas swept up from the ISM by the OB association in the vicinity.

References

Axon, D.J., Ellis, R.S. 1976, Mon. Not. R. astr. Soc., 177, 499.

Bastien, P., 1987, ApJ, 317, 231.

Bertoldi, F., 1989, ApJ, 346, 735.

Bertoldi, F., McKee, C.F., 1990, ApJ, 354, 529.

Bhatt, H.C., 1993, Mon. Not. R. astr. Soc., 262, 812.

Bhatt, H.C., 1995, unpublished.

Block, D.L. 1992, ApJ, 390, L13.

Boulares, A., Cox, D.P. 1990, Ap. J., 365, 544.

Goodman, A.A., Myers, P.C., Bastien, P. 1990, in Fragmentation of Molecular Clouds and Star Formation, eds. E.Falgarone, F.Boulanger, G.Duvert., Kluwer, Dordecht.

Greenberg, J.M. 1978, in Cosmic Dust, eds. McDonnell, J.A.M., Wiley, Chichester, p.187.

Gyulbudagyan, A.L. 1985, Astrofizica, 23, 295.

Heiles, C. 1995, in The Physics of the Interstellar medium and Intergalactic medium, eds A.Ferrara, C.F.McKee, C.Heiles and P.R.Shapiro, ASP conference series, Vol.80.

Heiles, C., Goodman, A.A., McKee, C.F., Zweibel, E.G. 1990, in Fragmentation of Molecular Clouds and Star Formation, eds. E.Falgarone, F.Boulanger, G.Duvert., Kluwer, Dordecht.

Heiles, C., Jenkins, E.B. 1976, Astr. Astrophys., 46, 333.

Hodapp, K.-W. 1987, ApJ, 319, 842.

Hsu,J.C. Breger, M. 1982, ApJ, 262, 732.

Indrani, C., Sridharan, T.K. 1994, JA&A, 15, 157.

Jain, S.K., Srinivasulu, G. 1991, Opt. Eng., 30, 1415.

Kahn, F.D. 1958, Rev. Mod. Phys., 30, 1058.

Kulkarni, S.R., and Heiles, C. 1987, in Galactic and Extragalactic Radio Astrono my, ed. K.I Kellerman and G.L Verschuur. (New York:Springer-Verlag), pp. 95-153.

Leung, C.M. 1985, in Protostars and Planets II, Ed. D.C.Black and M.S.Matthews, The University of Arizona Press, p,124.

Mathewson, D.S., Ford, V.L., 1970, Mon. Not. R. astr. Soc., 74, 139.

Parker, E.N. 1979, Cosmical Magnetic Fields, Oxford University Press.

Patel, N.A., Xie, T., Goldsmith, P.F. 1993, ApJ, 413, 593.

Pettersson, B. 1987, Astr. Astrophys. Supp., 70, 69.

Pettersson, B. 1991, in Low Mass Star Formation in Southern Molecular Clouds, Ed.B.Reipurth, ESO Scientific Report No. 11, p.69.
Pikelner, S.B., Sorochenko, R.L. 1974, Soviet Astr.–AJ, 17, 443.
Purcell, E.M. 1979, Ap. J., 231, 404.
Ramesh, B. 1995, Mon. Not. R. astr. Soc., 276, 923.
Reipurth, B. 1983, Astr. Astrophys., 117, 183.
Sahu, M., Pottasch, S.R., Sahu, K.C., Wesselius, P.R., Desai, J.N. 1988, Astr. Astrophys., 195, 269.
Sahu, M. 1992, Ph.D. Thesis, University of Groningen
Sahu, M., Sahu, K.C. 1992, Astr. Astrophys., 259, 265.
Scarrot, S.M., Draper, P.W., Rolf, C.D., Wolstencroft, R.D., 1992, Mon. Not. R. astr. Soc., 257, 485.
Schneps, M.H., Ho, P.T.P, Barret, A.H. 1980, ApJ, 240, 84.
Serkowski, K. 1974, in Planets, stars and nebulae studied with photopolarimetry, ed. Gehrels, T., University of Arizona Press, Tucson, p135.
Spitzer, L.Jr. 1978, Physical Processes in the Interstellar Medium (New York:Wiley-Interscience).
Sridharan, T.K. 1992a, JA&A, 13, 217.
Sridharan, T.K. 1992b, Ph.D Thesis, Indian Institute of Science, Bangalore.
Sugitani, K., Fukui, Y., Ogura, K. 1991, ApJ Supp., 77, 59.
Zealey, W.J., Ninkov, Z., Rice, E., Hartley, M., Tritton, S.B. 1983, Astrophys. Lett., 23, 119.
Zweibel, E.G., Heiles, C. 1997, Nature, 385, 131.